Binding of Tetracyclines to Elongation Factor Tu, the Tet Repressor, and the Ribosome: A Molecular Dynamics Simulation Study[†]

Alexey Aleksandrov and Thomas Simonson*

Laboratoire de Biochimie (CNRS UMR7654), Department of Biology, Ecole Polytechnique, 91128 Palaiseau, France

Received September 10, 2008; Revised Manuscript Received October 28, 2008

ABSTRACT: Tetracycline (Tc) is a broad-spectrum antibiotic that kills bacteria by interrupting protein biosynthesis. It is thought that the bacteriostatic action of Tc is associated with its binding to the acceptor site (or A site) in the bacterial ribosome, interfering with the attachment of aminoacyl-tRNA. Recently, however, the crystal structure of a complex between Tc and trypsin-modified elongation factor Tu (tm-EF-Tu) was determined, raising the question of whether Tc binding to EF-Tu has a role in its inhibition of protein synthesis. We address this question using computer simulations. As controls, we first compute relative ribosome binding free energies for seven Tc variants for which experimental data are available, obtaining good agreement. We then consider the binding of Tc to both the trypsin-modified and unmodified EF-Tu−GDP complexes. We show that the direct contribution of EF-Tu to the binding free energy is negligible; rather, the binding can be solely attributed to interactions of Tc with a bridging Mg^{2+} ion and the GDP phosphate groups. The effects of trypsin modification are modest. Further, our calculations show that EF-Tu does not exhibit any binding preference for Tc over the nonantibiotic, 4-dedimethyl-Tc, and EF-Tu does not bind the Tc analogue tigecycline, which is a potent antibiotic. In contrast, both the ribosome and the Tet Repressor protein (involved in Tc resistance) do show a binding preference for Tc over 4-dedimethyl-Tc, and the ribosome prefers to bind tigecycline over Tc. Overall, our results provide insights into the binding properties of tetracyclines and support the idea that EF-Tu is not their primary target.

Tetracycline (Tc)[1] is a broad-spectrum antibiotic, with activity against a wide range of Gram-positive and Gram-negative bacteria (*1*−*3*). Tetracyclines also have diverse applications in molecular biology and biotechnology, being used in conjunction with the Tet Repressor protein to artificially control the expression of target genes (*4*−*6*). In addition, they have a range of interesting, nonantibiotic properties; for example, they bind to and inhibit several human enzymes (*7, 8*). The bacteriostatic action of tetracycline has been extensively studied over the past 50 years, and it is well-established that Tc blocks protein biosynthesis (*9, 10*). Tc is thought to prevent the binding of aminoacylated tRNA to the A-site of mRNA-programmed ribosomes (*3*). Thus, the primary molecular target of Tc is thought to be the ribosome. Two structural studies in which Tc was diffused into pregrown crystals of the 30S ribosomal subunit identified two and six binding sites in which Tc makes direct contacts with rRNA (*11, 12*). Recently, we reported a computational study of Tc binding to the ribosome (*13*). Molecular dynamics and continuum electrostatic methods were employed, providing evidence that one site is predominant, consistent with its higher crystallographic occupancy in the X-ray structures. In this binding site, Tc primarily interacts with the H34 region of the 16S rRNA (*11, 12*), which is involved in the binding of aminoacyl-tRNA. This suggests further that this site is the primary target of Tc action. However, another possibility was suggested when Tc was shown to crystallize as a 1:1 complex with the trypsin-modified form of *Escherichia coli* EF-Tu−Mg−GDP (*14*). Thus, EF-Tu might be one of several Tc targets. Several classes of antibiotics exist that bind to EF-Tu and block protein synthesis (*15*−*17*). The structure of the tm-EF-Tu−Mg−GDP−Tc complex was recently reported (*18*), showing that Tc not only binds to tm-EF-Tu−Mg−GDP but does so by interacting with an important structural motif that is shared by all GTPases and many ATPases (*18*). Trypsin-modified EF-Tu lacks amino acids 45−58, which form the switch I loop, as well as residues 1−7. Heffron et al. (*18*) modeled the missing switch I loop into the tm-EF-Tu−Mg−GDP−Tc complex and found steric contacts between the loop and Tc, which might alter or impair Tc binding to intact EF-Tu. They also noted that the switch I loop is flexible, so that these contacts might be absent or relieved in the intact EF-Tu−Mg−GDP−Tc complex.

To clarify the possible biological relevance of Tc−EF-Tu binding, we use molecular dynamics and free energy simulations (*19*−*24*). Such calculations have become possible because we recently developed the first high-quality force

[†] Support was provided by the Nuclear Toxicology program of the Commmissariat pour l'Énergie Atomique and the Centre National pour la Recherche Scientifique (to T.S.). An Egide Ph.D. fellowship was awarded to A.A. Some of the simulations were performed at the CINES supercomputing center of the French Ministry of Education.

* To whom correspondence should be addressed. E-mail: thomas.simonson@polytechnique.fr. Phone: +33/169334860. Fax: +33/169334909.

[1] Abbreviations: EF-Tu, elongation factor Tu; TetR, Tet Repressor; Tc, tetracycline; 4-ddma-Tc, 4-dedimethyltetracycline; tRNA, transfer ribonucleic acid; GDP, guanosine diphosphate; PDB, Protein Data Bank; MD, molecular dynamics; MDFE, molecular dynamics free energy; PBFE, Poisson−Boltzmann free energy; PB/LRA, Poisson−Boltzmann linear response approximation; PME, particle mesh Ewald.

10.1021/bi801726q CCC: $40.75
Published on Web 11/25/2008

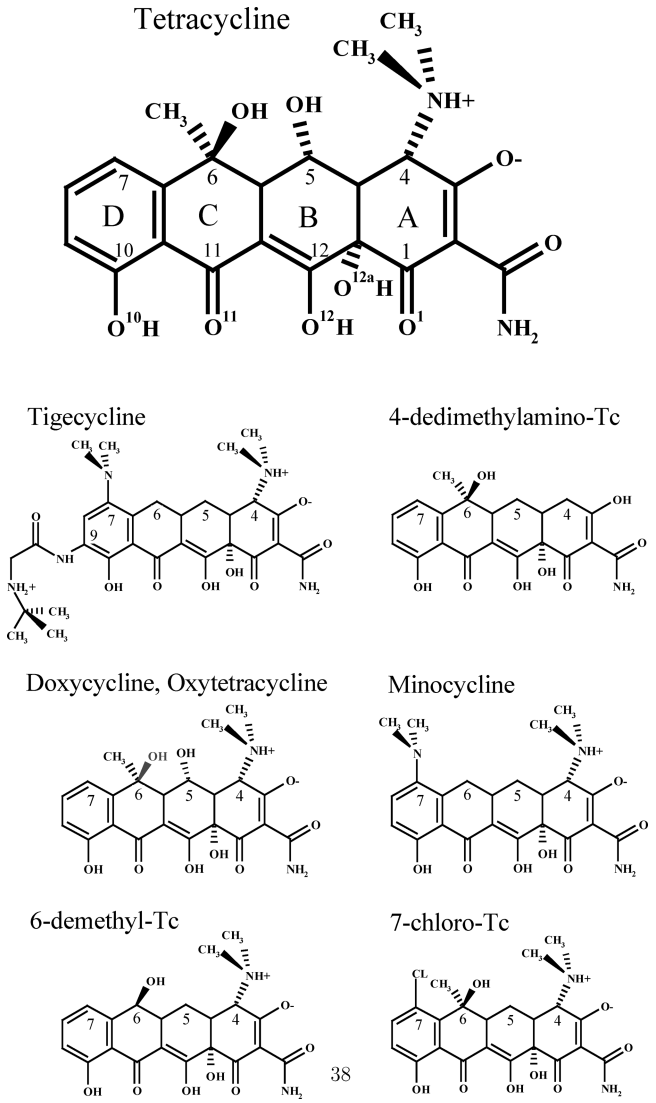

FIGURE 1: Plain tetracycline (Tc) and the seven analogues considered in this work.

field model for tetracycline and 11 of its analogues (*25, 26*). As a first step, we perform a series of control calculations, considering ribosome binding by Tc and several analogues for which experimental data are available (*27*−*31*). We use alchemical, molecular dynamics free energy simulations (MDFE) to compute the relative binding free energies, obtaining good agreement with experiment. Next, we consider both intact and tm-EF-Tu and their binding by Tc and two of its analogues: the potent antibiotic tigecycline and the nonantibiotic 4-dedimethyl-Tc (Figure 1). We compare the binding to EF-Tu, the ribosome, and the Tet Repressor (TetR), which mediates the main mechanism of Tc resistance. We show that when Tc binds to the EF-Tu−GDP−Mg complex, the contribution of EF-Tu to the binding free energy is negligible; rather, the favorable binding free energy can be solely attributed to interactions of Tc with the Mg^{2+} ion and the GDP phosphate groups. Results for intact and tm-EF-Tu are very similar. Further calculations show that EF-Tu does not exhibit any preference for Tc binding over the nonantibiotic analogue, 4-dedimethyl-Tc (4-ddma-Tc). In contrast, the ribosome does show a marked preference for Tc binding. We also performed free energy simulations to compare EF-Tu binding of Tc and its analogue tigecycline. Tigecycline is found to bind much more weakly to EF-Tu than Tc. Finally, we examined the G1058C mutation in the ribosome, which is known to produce Tc resistance (*27*). This mutation is shown to increase the Tc binding free energy, weakening binding. Along with recent results for Tc−ribosome binding and TetR induction by Tc (*13, 26, 32*), these data illustrate the modular structure of tetracyclines. Indeed, these molecules have one edge that primarily confirms receptor binding specificity, and another edge that controls metal binding and positioning, and can be used to act, through the metal ion, on a given environment (*26*). Overall, our results strongly support the idea that the ribosome, not EF-Tu, is the primary target of tetracycline.

MATERIALS AND METHODS

Computed Structures and Free Energies for EF-Tu−Tc Binding. (i) Molecular Dynamics Simulations. Crystal structures of elongation factor Tu (EF-Tu) were taken from Protein Data Bank (PDB) entries 1DG1 (intact EF-Tu without Tc) and 2HCJ (tm-EF-Tu with Tc bound) (*18, 33*). The simulations included protein residues within a 26 Å sphere, centered on the Tc binding site. In addition to crystal waters, a 26 Å sphere of water was overlaid and waters that overlapped protein, GDP, crystal waters, Tc (when present), or Mg^{2+} were removed. For the complexes of Tc with intact EF-Tu, the missing residues of the switch I loop (amino acids 45−58) and neighboring amino acids (41−44) were positioned on the basis of the 1DG1 structure; one side chain that overlapped Tc was manually reoriented, and the structure was energy-minimized with harmonic restraints applied to the entire protein except the loop. Throughout all the MD simulations, protein atoms between 20 and 26 Å from the sphere's center were harmonically restrained to their experimental positions. Simulations were conducted with the SSBP solvent model (*34*−*36*), which treats the region outside the 26 Å sphere as a uniform dielectric continuum, with a dielectric constant of 80. This is reasonable, since most of the outer region is water. Newtonian dynamics were used for the innermost region, within 20 Å of the sphere's center; Langevin dynamics were used for the outer part of the sphere, with a 292 K bath. The CHARMM22 force field was used for the protein (*37*) and the TIP3P model for water (*38*). Tc was described with the force field developed previously (*25*). The analogues tigecycline and 4-ddma-Tc were parametrized in a similar way (*26*). Electrostatic interactions were computed without any cutoff, using a multipole approximation for distant groups (*39*). Calculations were conducted with CHARMM (*40*). The same MD protocols were used for the class D Tet Repressor (TetR) and the *Thermus thermophilus* 30S ribosomal particles; see refs *13* and *32* for more details. Notice that there are a few nonstandard nucleotides in the *T. thermophilus* 30S ribosomal particle (*41*). Only two are within 12 Å of either Tc binding site. m^2Gua966 has a methyl group ~11 Å from the nearest Tc atom in TET1, pointing away from the ligand; m^5Cyt967 is somewhat closer, with its additional methyl ~6 Å from the acetamide nitrogen of Tc in the TET1 site (bottom right atom in the Figure 1 orientation). In the absence of force field parameters for m^5Cyt, we replaced both nucleotides with standard nucleotides, assuming that the additional methyl groups do not significantly affect the relative binding affinities of the various Tc variants. This should be reasonable, since the Cyt-

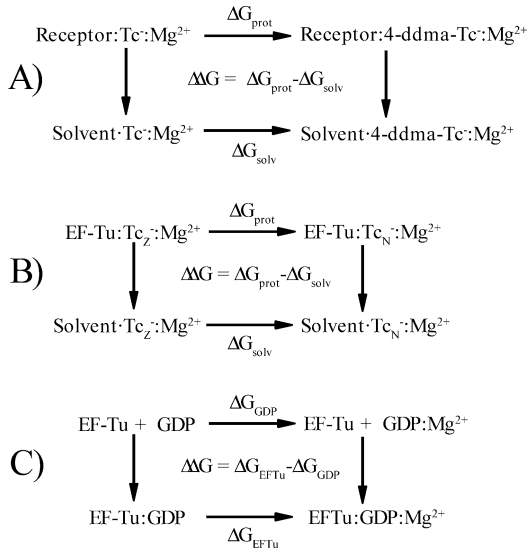

FIGURE 2: Thermodynamic cycles for ligand−receptor binding. (A) Comparing Tc and 4-ddma-Tc. Vertical legs represent $Tc^{-}-Mg^{2+}$ or 4-ddma-$Tc^{-}-Mg^{2+}$ species binding to a receptor (TetR, EF-Tu, or ribosome). Horizontal legs represent the alchemical transformation of Tc^{-} into 4-ddma-Tc^{-} in solution (below) or in the receptor$-Tc^{-}-Mg^{2+}$ complex (above). (B) Comparing Tc tautomeric states. (C) GDP−EF-Tu binding with and without cobound Mg^{2+}.

967 methyl is 6 Å distant and the Tc variants all share the exact same chemistry in the vicinity of their acetamide group (Figure 1).

(ii) Alchemical MD Free Energy (MDFE) Simulations. To compare Tc and a Tc analogue (i.e., Tc′) binding to a receptor (TetR, EF-Tu, or the ribosome), we use the thermodynamic cycle in Figure 2A. The MDFE method follows the horizontal legs of the cycle. Tc is reversibly transformed into its analogue during a series of MD simulations. The corresponding work is derived from a thermodynamic integration formula (*42*).

Most of the simulations were performed with the spherical boundary conditions described above (see also refs *43* and *44*): we considered receptor atoms within a sphere with a 25 Å radius, centered on an Mg^{2+} ion that coordinates tetracycline in TetR, EF-Tu, or the ribosome. However, the Tc/4-ddma-Tc transformations in the TetR protein and the ribosome were performed using a cubic box with a 74 Å edge. For these simulations, periodic boundary conditions were assumed and electrostatic interactions were approximated by the particle mesh Ewald (PME) method (*45*); as before, portions of the receptor more than 25 Å from the Mg^{2+} were neglected, and receptor atoms between 20 and 25 Å were harmonically restrained.

For the lower leg of the thermodynamic cycle, we simulate the $Tc-Mg^{2+}$ complex in solution. For the upper leg, we simulate a portion of the $Tc^{-}-Mg^{2+}$−receptor complex ($Tc^{-}-Mg^{2+}$−EF-Tu or $Tc^{-}-Mg^{2+}$−ribosome), solvated by the same 25 Å sphere or 74 Å water box. In each simulation system, the energy function can be expressed as a linear combination of $Tc^{-}-Mg^{2+}$ and $Tc'^{-}-Mg^{2+}$ terms:

$$U(\lambda) = U_0 + (1-\lambda)U(\mathrm{Tc}) + \lambda U(\mathrm{Tc}') \qquad (1)$$

where λ is a "coupling parameter" and U_0 represents interactions between parts of the system other than Tc. The free energy derivative with respect to λ has the form

$$\frac{\partial G}{\partial \lambda}(\lambda) = \langle U(\mathrm{Tc}') - U(\mathrm{Tc}) \rangle_{\lambda} \qquad (2)$$

where the brackets indicate an average over an MD trajectory with the energy function $U(\lambda)$ (*42, 23*). We gradually mutated Tc into Tc′ by changing λ from 1 to 0. The successive values of λ were 0.999, 0.99, 0.95, 0.9, 0.8, 0.6, 0.4, 0.2, 0.1, 0.05, 0.01, and 0.001. The free energy derivatives were computed at each λ value from a 100 ps MD simulation, or "window"; the last 80 ps of each window was used for averaging. A complete mutation run thus corresponded to 12 windows and 1.2 ns of simulation. Usually, one run was performed in each direction (Tc into Tc′ and the reverse).

Accurate uncertainty estimation with MDFE is difficult and expensive (*46*−*48*). A widely used approach is to perform multiple runs and measure the dispersion between runs. While this seems plausible, it neglects some forms of systematic error and can actually lead to an overestimated uncertainty. In particular, it is well-known that runs performed in opposite directions ("forward" and "backward" transformations; λ increasing or decreasing) exhibit systematic hysteresis effects (*49*−*51*). Thus, in the past, we have used error estimators that consider pairs of runs, one in each direction, forming a "forward/backward pair" (*43, 44, 52*). The forward/backward averages were much more reproducible than the individual values. Here, we use a variant of this approach. For most of the transformations considered, we performed a single pair of runs, one in each direction. For a given run, we split each trajectory window (corresponding to a particular λ value) into two halves; each collection of "half-windows" can be viewed as a "half-run". A forward and a backward half-run are viewed as a pair of runs, and the corresponding ΔG values are averaged. In this way, starting from one forward and one backward run, we obtain four half-runs and two averaged ΔG values. The uncertainty is taken to be their difference (i.e., two standard deviations). In practice, this method is roughly equivalent to estimating the uncertainty by block-averaging a single run (*53, 54*) and assuming systematic hysteresis effects mostly cancel whenever a forward and a backward run are averaged. To test this idea, we performed several pairs of forward/backward runs for two of the larger transformations (Tc vs 4-ddma-Tc, binding to TetR and to the ribosome). In both cases, the dispersion of the forward/backward averages was close to the uncertainty estimated by the previous method. The error estimated from the mean hysteresis (the difference between a forward and a backward run) was also not much greater; see the Supporting Information for details.

(iii) Poisson−Boltzmann Linear Response Approximation (PB/LRA). A recently developed method that combines MD simulations with continuum electrostatics is the Poisson−Boltzmann linear response approximation, or PB/LRA (*24, 32, 55*−*57*). This method is well-suited to treating rearrangements of atomic charges, as in the Tc_N to Tc_Z transformation. The free energy change (ΔG_{prot} and ΔG_{solv} in Figure 2B) is approximated by the continuum electrostatic free energy, averaged over the equilibrium states before and after the rearrangement. We applied the method using MD structures of the $Tc_N^{-}-Mg^{2+}$ and $Tc_Z^{-}-Mg^{2+}$ states (see above). We averaged free energies over 250 structures from the last 1 ns of the MD simulations.

Table 1: MD Free Energy Simulations for Tc Analogues Binding to the Ribosome

Tc analogue	ΔG_{rib}[a] (kcal/mol)	ΔG_{sol}[a] (kcal/mol)	$\Delta\Delta G$ (kcal/mol)	$\Delta\Delta G_{expl}$ (kcal/mol)
minocycline	−17.2 (1.1)	−15.0 (0.4)	−2.2 (1.2)	−2.6(*30*)
doxycycline	25.2 (0.4)	25.0 (0.3)	0.2 (0.5)	0.0(*27*), 0.2(*31*)
tigecycline	−112.3 (0.8)	−111.5 (0.7)	−0.8 (1.0)	−1.0(*29*), −1.1(*30*)
oxytetracycline	7.4 (0.2)	7.0 (0.3)	0.4 (0.4)	0.0[b](*28*)
6-demethyl-Tc	8.4 (0.2)	8.9 (0.2)	−0.5 (0.3)	NA
chlortetracycline	5.0 (0.2)	5.1 (0.2)	0.1 (0.3)	−0.4[b](*28*)
4-ddma-Tc	−25.9 (1.0)	−28.8 (0.6)	4.0 (1.1)	no binding[c]

[a] Columns 2 and 3 are the free energies for reversibly going from plain Tc to one of its analogues, either in the ribosome (ΔG_{rib}) or in solution (ΔG_{sol}). $\Delta\Delta G = \Delta G_{rib} - \Delta G_{sol}$ is the relative binding free energy. A negative $\Delta\Delta G$ means the Tc analogue binds more strongly. MDFE error bars are given in parentheses. [b] Derived from minimum inhibitory concentrations in vivo. [c] No observable binding (*60*).

RESULTS

Control Calculations: Ribosome Binding by Tc Variants. We considered ribosome binding by eight Tc variants, shown in Figure 1. Experimental data are available for plain Tc and six of the variants (Table 1). The relative binding free energies were computed through alchemical, molecular dynamics free energy simulations (termed MDFE) (*20, 23, 42, 58, 59*). Earlier computational work strongly suggests that Tc binds to the ribosome in its zwitterionic form, predominantly in the primary, TET1 site in the 30S subunit, stabilized by contacts between its cobound Mg^{2+} and three phosphate groups (*11, 13*). We assume the other seven ligands bind in the same manner. The simulations follow the horizontal legs of the thermodynamic cycle in Figure 2A, alchemically transforming the ligand from one Tc variant into another. The corresponding work is obtained from a thermodynamic integration formula (see Materials and Methods). Results are summarized in Table 1. More details on convergence and uncertainty are given in the Supporting Information. For two ligands (chlortetracycline and oxytetracycline), the experimental data have the form of in vivo minimum inhibitory concentrations (*28*), which provide only a qualitative test. For one other ligand (6-demethyl-Tc), no experimental data are available. For 4-ddma-Tc, there is no observable binding (*60*), which is consistent with the large, positive, computed $\Delta\Delta G$. Overall, the calculations agree very well with experiment. This indicates that the force field is accurate and the MDFE protocol is reasonable. Both the force field and the MDFE methodology have been further tested in the past (*23, 26, 32*).

Analysis of the Experimental Structures of EF-Tu with and without Tc. A recently published X-ray structure (*18*) revealed that Tc binds on the surface of domain 1 of the tm-EF-Tu−GDP complex, as shown in Figure 3A. Tc's phenol-diketone moiety interacts directly with the Mg^{2+} ion in the GTPase active site of tm-EF-Tu (Figure 3B). O12a of Tc interacts with the phosphate group of GDP. Thr25 coordinates the Mg^{2+} ion through its hydroxyl group; Asp80 also interacts with the Thr25 hydroxyl group. Tc does not interact directly with either side chain; the distance between the Asp80 oxygen and the Thr25 oxygen is 2.6 Å, whereas the Tc oxygen, O10, is 3.3 Å distant. To interact with Asp80, which is out of the plane of the D ring of Tc, the Tc hydrogen of the O10 hydroxyl group would have to be rotated by 90° out of plane, which is very unfavorable (for the hydroxyl group of phenol, the rotation barrier is ∼3 kcal/mol) (*61*). The second oxygen of Asp80 makes a hydrogen bond to Thr16 and to a water molecule that coordinates the Mg^{2+} ion (water W1 in Figure 3B). No hydrogen bonds are apparent between Tc and any residues of EF-Tu. Tc replaces two well-ordered water molecules found in the Mg^{2+} coordination sphere in all other EF-Tu structures (*18*). Overall, the Mg^{2+} ion is coordinated by two water molecules, the Thr25 oxygen, two oxygens of Tc, and one oxygen of the terminal phosphate group of GDP. Superposition of the EF-Tu−GDP complex with and without Tc (PDB entry 1DG1) shows that there are no significant conformational changes upon Tc binding (see Figure 3A). The root-mean-square deviation (rmsd) between the two structures for the backbone atoms within a 10 Å sphere around GDP is just 0.3 Å; for the GDP atoms, the rms deviation is also 0.3 Å.

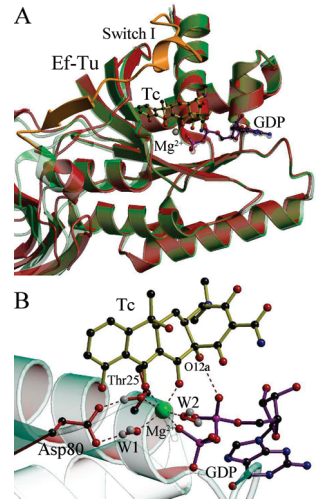

FIGURE 3: (A) Superposition of the X-ray structures of EF-Tu with (red) and without (green) bound Tc, showing that there are no large conformational changes upon Tc binding. The modeled switch I loop is shown for the holo structure (orange), after relaxation by molecular dynamics, which leads to a 2 Å rms shift (see the text). (B) Close-up view of the Tc binding site, showing that there are no hydrogen bonds between Tc and EF-Tu.

Analysis of the Structures from the Simulations. The complexes between Tc in its zwitterionic tautomer and either intact or tm-EF-Tu were each simulated by molecular dynamics (MD) for 4 ns. The structures sampled in the simulation are in good agreement with the X-ray structure. The rms deviation, averaged over the last 1 ns of dynamics and over backbone atoms, is 0.6 Å; the average for non-hydrogen atoms within 10 Å of Tc is 0.9 Å. The EF-Tu ligands, Mg^{2+}, GDP, and Tc all maintain their positions relative to the X-ray structure. Mg^{2+} coordinates OG1 of Thr25, a phosphate oxygen of GDP, and two oxygens of Tc and engages in water-mediated interactions with Asp80 throughout the MD simulation. Tetracycline does not make direct hydrogen bonds to EF-Tu; the 4-dimethylamino and 3-enolate groups of Tc ring A, which are important for its antibiotic function (discussed below), are completely solvent-exposed.

In the intact EF-Tu−GDP−Tc complex, after 2 ns of dynamics, the Tc ligand has shifted with respect to its starting position by ∼1 Å, while residues 41−58 of the switch I loop have shifted by 2 Å. Most of this shift has already occurred after the initial energy minimization of the loop (see Materials and Methods); the deviation does not increase

during the last 2 ns of dynamics. Notice that the switch I loop is not strongly anchored to the rest of the EF-Tu structure and is able to shift considerably between the GDP and GTP states (by more than 20 Å) (*18*). In the holo MD structure, after 2 ns of dynamics, there are no hydrogen bonds between Tc and residues 41−58, and very few van der Waals contacts. The shortest Tc−loop distances are between the Ile49 and Phe46 side chains and the Tc 4-dimethyl groups (3.5 and 3.9 Å, respectively) and between the Asp50 OD1 atom and C4 in Tc (3.7 Å). All other distances are greater than 4 Å. The Asp50 side chain is fully exposed to solvent, so that its charge is shielded.

Mg^{2+} Stabilizes the EF-Tu−GDP Complex. In the EF-Tu−GDP crystal structure without Tc, an Mg^{2+} ion is present (*18*). As a first step, we examine here its role in GDP binding to EF-Tu. This step is needed for the analysis of Tc binding below. We use MDFE simulations where the Mg^{2+} ion is gradually introduced, either in complex with GDP or in the protein, according to the thermodynamic cycle in Figure 2C. In principle, these simulations should allow us to compute the relative free energies for GDP−EF-Tu binding, with and without a cobound Mg^{2+}. In practice, we employ a so-called "fixed-charge" force field: atomic charges have fixed values, and the electronic polarization of water, GDP, or protein by the divalent Mg^{2+} is not explicitly modeled (see Materials and Methods). A consequence is that the force field cannot provide very accurate binding thermodynamics for reactions involving Mg^{2+}. However, it can still give useful information about the incremental contribution of Mg^{2+} to GDP−EF-Tu binding. Indeed, in the protein complex, the Mg^{2+} charge is shielded and neutralized by the GDP phosphate groups. Furthermore, the Mg^{2+} ion does not interact closely with highly polarizable protein groups. Its octahedral coordination sphere includes only one EF-Tu atom, OG1 of Thr25 (Figure 3). Thus, any force field artifacts should be fairly small when we consider the incremental effect of Mg^{2+} on EF-Tu−GDP binding.

We therefore consider the thermodynamic cycle in Figure 2C. In the vertical legs, GDP binds to EF-Tu. The horizontal legs introduce Mg^{2+}, to form a complex either with GDP (upper leg) or with EF-Tu−GDP (lower leg). We assume that the allosteric, structural changes associated with EF-Tu−GDP binding are the same, whether or not Mg^{2+} is cobound to GDP. With this assumption, we can limit our analysis to the GDP-bound conformation of EF-Tu. Indeed, we may assume that to bind GDP, apo-EF-Tu is first brought into this conformation. The free energy to do this cancels, when the left- and righthand legs of the thermodynamic cycle are compared. Therefore, the allosteric changes do not play a role when the incremental effect of Mg^{2+} on GDP binding are analyzed.

The free energies of the horizontal legs are calculated by MDFE, giving a $\Delta G_{\text{Ef-Tu}}$ of -492.5 ± 2.0 and a ΔG_{GDP} of -478.3 ± 6.0 kcal/mol (notations are defined in Figure 2C). The difference between the introduction of Mg^{2+} into the protein and into the GDP complex is $\Delta\Delta G = \Delta G_{\text{Ef-Tu}} - \Delta G_{\text{GDP}} = -14.2$ kcal/mol. Thus, binding of Mg^{2+} to GDP−EF-Tu is much stronger than binding of Mg^{2+} to GDP alone. Most importantly, $\Delta\Delta G$ can be interpreted as the difference in GDP binding free energies in the presence and absence of the Mg^{2+} ion. We see that in the absence of Mg^{2+}, binding of GDP to EF-Tu is much less favorable. Indeed, it was found experimentally that removing Mg^{2+} from EF-Tu−GDP accelerates the dissociation of GDP by a factor of 150−300 (*62*). Therefore, we may conclude that GDP always binds to EF-Tu with a cobound Mg^{2+} ion, consistent with the GDP−EF-Tu X-ray structure (*18*); the population of complexes with no cobound Mg^{2+} is predicted to be infinitesimally small. In what follows, we will therefore assume that in EF-Tu, when GDP is present, Mg^{2+} is always cobound.

Table 2: PB/LRA Free Energy Simulations Comparing Binding of Tc_N^- and Tc_Z^- to EF-Tu[a]

	$\varepsilon_P = 1$	$\varepsilon_P = 2$
$\Delta G_{\text{protein}}$	55.9 (0.4)	28.0 (0.2)
$\Delta G_{\text{solvent}}$	55.8 (0.5)	27.9 (0.3)
$\Delta\Delta G$	0.1 (0.6)	0.1 (0.4)

[a] Energies in kilocalories per mole; uncertainties are in parentheses. $\Delta G_{\text{protein}}$ and $\Delta G_{\text{solvent}}$ correspond to the alchemical transformation of Tc from one form into the other. $\Delta\Delta G = \Delta G_{\text{protein}} - \Delta G_{\text{solvent}}$ is the binding free energy difference. $\Delta\Delta G$ is very small, indicating that EF-Tu does not discriminate between the zwitterionic and neutral forms of Tc.

Tc Binds to EF-Tu in Its Zwitterionic Form. As a second step, we now establish which Tc tautomer is preferentially bound by the EF-Tu−GDP complex. We showed earlier that the preferred Tc tautomer in solution is the zwitterionic one, Tc_Z (*32*). Furthermore, both TetR and the ribosome bind more strongly to Tc_Z than to the neutral form, Tc_N (*13, 32*). Here, we compare Tc_N and Tc_Z binding to EF-Tu, using a Poisson−Boltzmann linear response approximation method (PB/LRA) (*24, 32, 55−57*). This method follows the horizontal legs of the thermodynamic cycle in Figure 2B: the Tc_N moiety is transformed into Tc_Z both in solution and in complex with the protein (see Materials and Methods). Notice that to bind Tc to the EF-Tu−GDP complex, an Mg^{2+} ion must first be removed from the protein (see above), since Tc brings its own Mg^{2+} with it. This step is the same for Tc_N and Tc_Z, so it does not play any role in the Tc_N versus Tc_Z comparison. Notice also that an Mg^{2+} ion is cobound to Tc both in solution and in the complex with EF-Tu−GDP; therefore, the reaction considered here does not require us to accurately describe the thermodynamics of Mg^{2+} binding and/or release (see the discussion in the previous section).

Structural ensembles for each state (Tc_Z or Tc_N) are obtained from MD simulations. The electrostatic potential on the ligand atoms is then computed using continuum electrostatics, by solving the Poisson−Boltzmann equation (see Materials and Methods). Finally, the potentials are combined with a linear response approximation to obtain a free energy change (*24, 32, 55−57*). Subtracting the two legs of the cycle yields the binding free energy difference, $\Delta\Delta G$. The Poisson−Boltzmann calculations are done with a low protein dielectric constant of either 1 or 2. This is the appropriate range for the present PB/LRA method (*24, 32, 55−57*), because most of the protein reorganization is explicitly modeled by performing MD simulations of the two end points (Tc_N and Tc_Z complexes). Results are summarized in Table 2. Both dielectric values lead to a $\Delta\Delta G$ of 0.1 kcal/mol, with an estimated uncertainty of approximately ±0.5 kcal/mol. This means that the EF-Tu−Mg−GDP complex does not exhibit any preference between the neutral and zwitterionic states of Tc. This contrasts with the Tet Repressor and the ribosome, both of

Table 3: Contributions of Selected EF-Tu Residues to the Tc Binding Free Energy[a]

residue	free energy contribution	residue	free energy contribution
Lys24	−9.0 (0.7)	Asp86	1.5 (0.8)
Asp21	2.1 (0.6)	Thr25	2.7 (0.8)
Asp80	7.8 (0.6)	GDP	25.1 (0.9)
		GDP−Mg^{2+}	−67.0 (1.0)
all protein residues together			0.9 (1.0)

[a] PB free energies are in kilocalories per mole; uncertainties are in parentheses. Only amino acids contributing more than 1 kcal/mol (in absolute magnitude) are shown. Calculations were conducted with a protein dielectric constant (ε_P) of 4.

which have a strong preference for Tc_Z binding. The lack of a preference can be explained by the fact that the 4-dimethylamino and enolate moieties of Tc are solvent-exposed in the EF-Tu complex (see Figure 3B) and do not interact directly with any protein residues or with GDP. The Tc_N versus Tc_Z stability difference in solution has been estimated quantum mechanically to be approximately −3 kcal/mol in favor of Tc_Z (*25, 63*); this means that Tc binds to EF-Tu in its zwitterionic form, even though EF-Tu itself does not discriminate between Tc_Z and Tc_N.

A Component Analysis of the Binding Free Energy between Tc and EF-Tu. We now turn to a group or "component" analysis of the Tc−EF-Tu binding free energy. This analysis will show that Tc binding is mainly promoted not by EF-Tu itself, but by the GDP-associated Mg^{2+} ion. MDFE and PB/LRA methods were used to compute binding free energy differences. A third method is used here, the Poisson−Boltzmann free energy method (PBFE) (*19, 21, 23, 24*). This method gives an estimate of the contribution of electrostatic interactions to the binding free energy, using the vertical legs of the thermodynamic cycle in Figure 2A (see Materials and Methods). The PBFE method is less rigorous than MDFE or PB/LRA; its advantage is that it provides an intuitive decomposition of the binding free energy into contributions from individual protein groups (*13, 23, 24, 64, 65*). PBFE involves a single adjustable parameter, the protein/ligand dielectric constant, ε_P. It is set here to 4, based on extensive applications to other protein−ligand complexes (*19, 21, 23, 24, 32*). This differs from the PB/LRA situation described above, where protein reorganization was explicitly modeled through MD simulations, so that a lower dielectric (1−2) was appropriate. For comparison, we also did calculations with an ε_P value of 8. Although the absolute magnitude of the group contributions varies with ε_P, the relative contributions of different groups, which are of interest here, are robust with respect to the choice of ε_P. We use the PBFE method to analyze binding of Tc_Z to the EF-Tu−GDP−Mg complex.

Results are summarized in Table 3. The overall binding free energies estimated for intact and tm-EF-Tu agree within 0.3 kcal/mol (not shown), so that only the data for tm-EF-Tu are given. The largest single-residue contribution to the binding free energy between Tc and EF-Tu comes from Lys24, which interacts directly with the terminal phosphate group of GDP. This is explained by the opposite charges on the negative Tc and the positive lysine, which prefers to interact with $[Tc-Mg]^+$, rather than Mg^{2+} alone. In contrast, interactions with Asp80, Thr25, Asp21, and Asp86 all favor binding of Mg^{2+} over $[Tc-Mg]^+$. Strikingly, the total contribution of all EF-Tu residues to the binding free energy of Tc is small (0.9 kcal/mol), within the ∼2 kcal/mol uncertainty of the PBFE method. As expected, the largest positive contribution comes from GDP, which is negatively charged, and prefers Mg^{2+} over $[Tc-Mg]^+$ binding. Overall, under the standard state conditions simulated here, it is the Mg^{2+} ion itself that is solely responsible for the binding of $[Tc-Mg]^+$, rather than Mg^{2+} alone, to EF-Tu. In the crystallographic experiment (*18*), Tc without any bound Mg^{2+} was diffused into the EF-Tu−GDP crystals. The Mg^{2+} concentration was thus substoichiometric with respect to Tc and GDP: there is not enough Mg^{2+} to saturate both the EF-Tu−GDP complex and any unbound Tc. Therefore, each Tc shares an Mg^{2+} ion with the EF-Tu−GDP complex, and the interactions with Mg^{2+} drive Tc binding. As the Mg^{2+} concentration becomes larger, unbound Tc becomes associated with Mg^{2+}, and Tc will not bind to EF-Tu. Overall, the lack of any intrinsic preference for $[Tc-Mg]^+$ over Mg^{2+} on the part of EF-Tu suggests that EF-Tu does not play the role of a specific Tc target.

Table 4: Binding Free Energy Differences ($\Delta\Delta G$) between Tc and the Nonantibiotic Analogue, 4-Dedimethylamino-Tc, for Tc Binding to EF-Tu, the Ribosome, and TetR[a]

target	$\Delta\Delta G_{comp}$	$\Delta\Delta G_{exptl}$
Tet Repressor	4.6 (1.6)	>5.0[b]
ribosome	4.0 (1.1)	NA[c]
EF-Tu−GDP	−0.9 (0.7)	NA[c]
tm-EF-Tu−GDP	−0.1 (0.6)	NA[c]

[a] Energies in kilocalories per mole. Uncertainties are in parentheses. A positive $\Delta\Delta G$ corresponds to preferential Tc binding. [b] Experiment only gives a lower bound (*2*). [c] Experimental values are not known.

Tc versus Nonantibiotic 4-Dedimethylamino-Tc Binding to the Ribosome, EF-Tu, and the Tet Repressor. The possible role of EF-Tu as a Tc target was analyzed further by comparing the binding of two Tc analogues, one of which is a potent antibiotic and the other a nonantibiotic. We first consider 4-dedimethylamino-Tc [4-ddma-Tc (Figure 1)], which is not an antibiotic (*60*). Additionally, compared to Tc, it has a much weaker binding affinity for the Tet Repressor (TetR), which is a part of the antibiotic resistance mechanism (*2, 66*). We test the competition between Tc and 4-ddma-Tc binding to EF-Tu, TetR, and the ribosome. We use MDFE simulations (see Materials and Methods), which do not involve any adjustable parameters (*23, 42, 59*). The simulations predict a Tc versus 4-ddma-Tc binding free energy difference for TetR of 4.6 ± 1.6 kcal/mol (Table 4). This is consistent with experiment, which indicates a binding free energy difference of ≥5.0 kcal/mol (*2*). Thus, 4-ddma-Tc binding is much weaker than Tc binding, mainly because of lost hydrogen bonds with His62, Asn82, and Gln116. Details about the convergence and uncertainty of the MDFE simulations are given in the Supporting Information.

The Tc versus 4-ddma-Tc free energy difference for ribosome binding was computed to be 4.0 ± 1.1 kcal/mol, strongly favoring Tc binding (Table 4). We attribute this result to the loss of hydrogen bonds between the Tc 4-amino group and the phosphate of Gua966, and to water-mediated interactions between Tc and rRNA. Indeed, we can decompose the free energy changes into components associated with the Coulomb electrostatic and van der Waals energy terms, respectively. Subtracting the results in solvent and the ribosome complex, we find that $\Delta\Delta G$ arises mostly from

Table 5: Binding Free Energy Differences ($\Delta\Delta G$) between Tc and the Potent Antibiotic Tigecycline for Tc Binding to EF-Tu and the Ribosome[a]

target	$\Delta\Delta G_{comp}$	$\Delta\Delta G_{exptl}$
EF-Tu−GDP	25.1 (2.0)	NA[b]
ribosome	–0.8 (1.0)	–1.0,[c] –1.1[c]

[a] Energies in kilocalories per mole. Uncertainties are in parentheses. A positive $\Delta\Delta G$ corresponds to preferential Tc binding. [b] Experimental value unknown. [c] Experimental values from refs *29* and *30*.

the Coulomb terms (2.5 kcal/mol), with a smaller van der Waals component (1.5 kcal/mol).

Finally, in contrast to TetR and the ribosome, the Tc versus 4-ddma-Tc free energy difference for EF-Tu binding was found to be small and negative [$\Delta\Delta G = -0.9 \pm 0.7$ kcal/mol for intact EF-Tu (favoring 4-ddma-Tc), and $\Delta\Delta G = -0.1 \pm 0.6$ kcal/mol for tm-EF-Tu (Table 4)]. The estimated uncertainty is consistent with the value that would be inferred from the 2 kcal/mol forward−backward hysteresis (±1 kcal/mol; data not shown). The small $\Delta\Delta G$ values arise because the 4-dimethylamino and 3-enolate groups of Tc are solvent-exposed in the complexes with EF-Tu and tm-EF-Tu (see Figure 3). The portion of Tc that binds directly to the EF-Tu−GDP−Mg complex is the same in Tc and 4-ddma-Tc. The slightly more negative value found for intact EF-Tu indicates that 4-ddma-Tc binding is actually a bit stronger than Tc binding; this may be due to a slight steric interference between the switch I loop and the dimethylammonium group of Tc, as suggested by Heffron et al. (*18*); indeed, with trypsin-modified EF-Tu, the switch I loop is absent, and the two ligands have essentially the same affinities. However, the difference between the two results is small (0.8 kcal/mol) and within the MDFE uncertainty. Thus, EF-Tu does not distinguish between the antibiotic Tc and the nonantibiotic 4-ddma-Tc; if anything, intact EF-Tu has a slight preference for the nonantibiotic. This appears to be inconsistent with a role for EF-Tu as a specific Tc target.

Tc versus Tigecycline Binding to the Ribosome and EF-Tu. Tigecycline, the 9-*tert*-butylglycylamido derivative of minocycline (Figure 1), is a broad-spectrum antibiotic that is not affected by classical Tc resistance mechanisms, including ribosomal protection and efflux by Tc-specific pumps (*67, 68*). Tigecycline was also found to bind 5 times more strongly than Tc to the ribosome (*29, 30*). Bauer et al. showed by Fe^{2+}-mediated cleavage that tigecycline binds to the same high-affinity site in the 16S rRNA as Tc (*69*). Here, we test the competition between Tc and tigecycline binding to EF-Tu and the ribosome using MDFE (see Materials and Methods). Results are summarized in Table 5. For ribosome binding, the simulations predict a Tc versus tigecycline binding free energy difference of -0.8 ± 1.0 kcal/mol, in good agreement with the experimental value of −1.0 kcal/mol (*29*). This value results from the attractive electrostatic interaction between the positively charged 9-*tert*-butylglycylamido group of tigecycline and the negative phosphate group of Ade1055 in the ribosome.

The same transformation was performed in EF-Tu. The computed binding free energy difference is extremely large, 25.1 ± 2.0 kcal/mol, showing that tigecycline does not bind to EF-Tu at all. More precisely, it cannot bind in the same manner as Tc; other binding sites and modes cannot be ruled out. The large $\Delta\Delta G$ value results from steric clashes between the 9-*tert*-butylglycylamido substituent of tigecycline and residues 62−65 and 80−82 of EF-Tu (see Figure 3A). If tigecycline and Tc share the same type of bacteriostatic function, this result strongly suggests that EF-Tu cannot be the primary target of Tc.

The Ribosome Resistance Mutation G1058C Reduces the Level of Tc Binding. As a final illustration of the properties of binding of Tc to the ribosome, we consider the effect of a resistance mutation on Tc binding. The G1058C mutation in the 16S rRNA was identified in clinical isolates of Tc-resistant Cutaneous Propionibacteria (*27*). This mutation was also found in isolates of *Brachyspira hyodysenteriae* that have increased minimal inhibitory concentrations (MICs) for doxycycline, another Tc analogue (*70*). The experimental binding free energy difference was estimated from the MICs to be 2.2 ± 1.0 kcal/mol (*27, 70*). We study the effect of the G1058C mutation on Tc binding. MD simulations were performed for both the wild-type ribosome−Tc^-−Mg^{2+} complex and the G1058C mutant (Figure 4). The binding free energy difference was then estimated by PBFE (see above). This method is less rigorous than the MDFE and PB/LRA methods used above. However, it should give a qualitative estimate of the binding free energy change. The simulation and PBFE setup were described previously (*13*) and in Materials and Methods. With a ribosome dielectric constant of 8, used previously (*13*), the computed binding free energy difference is 4.5 (0.7) kcal/mol, in rough agreement with the experimental value of 2.2 kcal/mol. With a somewhat higher dielectric of 12, we would obtain a value of 2.4 kcal/mol, close to the experimental value. Thus, the Tc resistance phenotype is reflected in the Tc binding properties of the ribosome. It is unclear whether the improved agreement with a dielectric of 12 is significant. With the higher dielectric, agreement for other, related binding properties is poorer (minocycline vs Tc ribosome binding) (*13*); also, the uncertainty of the PBFE method is higher than for the other methods used here (MDFE and PB/LRA), so that a difference of 2 kcal/mol between two model variants is less compelling. In the MD simulations, the G1058C mutation leads to rearrangements in helix 34 of the 16S RNA, which in turn affect the Mg^{2+} coordination (Figure 4) and lead to a decreased binding affinity for the Tc^-−Mg^{2+} complex. The Mg^{2+} ion that coordinates Tc also interacts with O1P of Cyt1054 in the wild-type ribosome, while in the G1058C mutant simulations, it loses this interaction and chelates O4′ of Cyt1054 instead. As a result, the Tc position is slightly rotated compared to its wild-type position (Figure 4).

CONCLUDING DISCUSSION

Tetracycline binding to protein and RNA is a complex process, involving a competition between several effects, with electrostatics playing an important role. This is illustrated by our earlier, detailed studies of ribosome and TetR binding. Protonation states of the protein and the ligand were determined, as well as TetR side chain orientations (*13, 32*). Similarly, it was necessary here to determine which Tc tautomer binds to EF-Tu and whether the Mg^{2+} ion is always prebound. Free energy simulations are a powerful technique for studying such complex processes, complementary to experiment. After an initial burst of popularity in the early

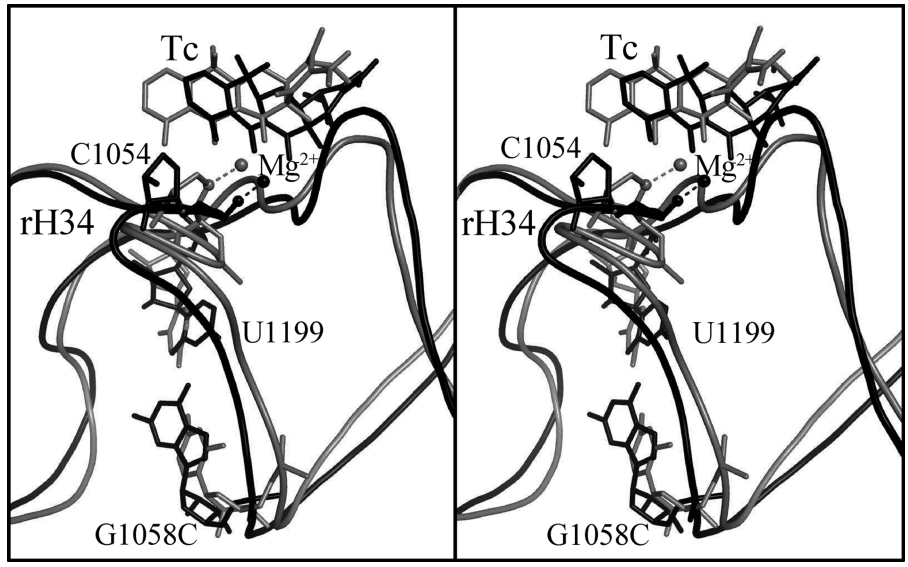

FIGURE 4: Native and mutant ribosome interacting with Tc. Divergent stereoview. The MD structure of Tc bound to the native ribosome is colored black; the G1058 mutant is colored gray. The Mg^{2+} ions are shown as spheres. Tetracycline and rRNA residues 1058, 1199, and 1054 are in stick representation. The O1P and O4 atoms of C1054 are shown as spheres in the black and gray structures, respectively.

1990s (*59*), technical and fundamental difficulties were brought to light that led to a decline in their use. In recent years, substantial progress has been made (*20, 23, 24, 71*), as illustrated here by the good agreement with experiment for our control calculations. Another major technical difficulty for simulation studies is the force field parametrization of Tc and its analogues, which must be done at a high level of accuracy. Our Tc parametrization (*25*) followed the same rigorous procedure that was used for the rest of the CHARMM force field (*37, 72*). The same procedure was used more recently to parametrize 11 other Tc analogues, including 4-ddma-Tc and tigecycline (*63*). This force field approach allows us to study both protein and nucleic acid binding with a comparable accuracy. Thus, we obtained good agreement with the experiments described above for Tc analogues binding to the ribosome; free energy calculations for several Tc analogues binding to TetR have given similar agreement (A. Aleksandrov and T. Simonson, unpublished data).

To test the hypothesis of a functional role for Tc−EF-Tu binding, we have compared the binding strength of Tc and two analogues: tigecycline, one of the most potent Tc antibiotics, and the nonantibiotic, 4-ddma-Tc. Removal of the 4-dimethylamino group of Tc (giving 4-ddma-Tc) abolishes all its antimicrobial properties, which underlines the functional importance of this group (*60*). The behavior of EF-Tu was compared to that of the ribosome, usually thought to be the primary biological target, and to that of the Tet Repressor, which mediates the primary mechanism of Tc resistance. With this approach, we have obtained evidence suggesting that although EF-Tu can bind Tc, it is not part of the Tc bacteriostatic mechanism. Indeed, Heffron et al. showed that Tc can bind to trypsin-modified EF-Tu (*18*), which lacks the switch I loop, but suggested that steric overlap between Tc and this loop might prevent Tc binding to intact EF-Tu. Here, we find that after several nanoseconds of molecular dynamics, there is no steric overlap between Tc and the switch I loop, and the Tc binding properties of intact and tm-EF-Tu are very similar. However, EF-Tu has a weak preference for 4-ddma-Tc over Tc and does not bind tigecycline at all. This contrasts directly with their relative antibiotic properties. The ribosome, on the other hand, has a strong binding preference for Tc over 4-ddma-Tc, and for tigecycline over Tc. The small difference between Tc and 4-ddma-Tc binding to EF-Tu is not surprising, given the X-ray structure, where Tc does not make any direct hydrogen bonds to EF-Tu. However, for a quantitative statement, these simulations were necessary. Furthermore, the simulations reveal that EF-Tu does not contribute directly to the Tc binding affinity; rather, binding of Tc to the EF-Tu−GDP−Mg complex is mediated by the Mg^{2+} ion. Overall, our results are consistent with a broad range of experimental data. They suggest that EF-Tu is not the primary target of Tc. Interestingly, TetR prefers to bind Tc over 4-ddma-Tc; this is reasonable, since TetR evolved under selective pressure for bacteria to resist the natural toxin, Tc, but not the recent, man-made analogue, 4-ddma-Tc. Similarly, TetR−tigecycline binding has not been optimized by natural selection, though tigecycline is thought to bind to TetR and induce the *tetR* and *tetA* genes (*3*).

These data illustrate further the modular structure of tetracyclines. Indeed, these molecules are seen to have a "specificity" edge that primarily confers receptor binding specificity (roughly, the upper edge in Figure 1) and another, "metal-display" edge that controls metal binding and positioning. Recent crystallographic and simulation studies (*13, 73, 74*) have shown that in the Tet Repressor protein, for example, the cobound, divalent magnesium ion is primarily responsible for driving the protein through its allosteric transition into the induced state; tetracycline itself mainly plays the role of an adaptor, or metal carrier. In the ribosome, we recently used a free energy decomposition analysis to show that Tc binding is mainly driven by magnesium−phosphate interactions; the specificity edge of Tc presumably serves to fine-tune the binding and make it specific. Here, we have an even more extreme example of the modular Tc structure: only the metal-display edge is used to bind EF-Tu; the metal itself contributes all of the affinity, and there is no specificity at all. In the future, these and

similar insights could help in the engineering of new antibiotics and new systems for gene regulation.

ACKNOWLEDGMENT

We thank Frances Jurnak and Winfried Hinrichs for discussions and Martin Karplus for CHARMM.

SUPPORTING INFORMATION AVAILABLE

Details of free energy simulations and their convergence. This material is available free of charge via the Internet at http://pubs.acs.org.

REFERENCES

1. Taubes, G. (2008) The bacteria fight back. *Science 321*, 356–361.
2. Lederer, T., Kintrup, M., Takahashi, M., Sum, P., Ellestad, G., and Hillen, W. (1996) Tetracycline analogs affecting binding to Tn10-Encoded Tet repressor trigger the same mechanism of induction. *Biochemistry 35*, 7439–7446.
3. Chopra, I., and Roberts, M. (2001) Tetracycline antibiotics: Mode of action, applications, molecular biology, and epidemiology of bacterial resistance. *Microbiol. Mol. Biol. Rev. 65*, 232–260.
4. Fussenegger, M. (2001) The impact of mammalian gene regulation concepts on functional genomic research, metabolic engineering, and advanced gene therapies. *Biotechnol. Prog. 17*, 1–51.
5. Berens, C., and Hillen, W. (2003) Gene regulation by tetracyclines: Constraints of resistance regulation in bacteria shape TetR for application in eukaryotes. *Eur. J. Biochem. 270*, 3109–3121.
6. Berens, C., Lochner, S., Lober, S., Usai, I., Schmidt, A., Drueppel, L., Hillen, W., and Gmeiner, P. (2006) Subtype selective tetracycline agonists and their application for a two-stage regulatory system. *ChemBioChem 7*, 1320–1324.
7. Pruzanski, W., Stefanski, E., Vadas, P., McNamara, T. E., Ramamurthy, N., and Golub, L. M. (1998) Chemically modified non-antimicrobial tetracyclines inhibit activity of phospholipases A_2. *J. Rheumatol. 25*, 1807–1812.
8. Hamdan, I. I., Afifi, F., and Taha, M. O. (2004) In vitro α amylase inhibitory effect of some clinically-used drugs. *Pharmazie 59*, 799–801.
9. Schnappinger, D., and Hillen, W. (1996) Tetracyclines: Antibiotic action, uptake, and resistance mechanisms. *Arch. Microbiol. 165*, 359–369.
10. Chopra, I., Hawkey, P. M., and Hinton, M. (1992) Tetracyclines, molecular and clinical aspects. *J. Antimicrob. Chemother. 29*, 245–277.
11. Brodersen, D. E., Clemons, W. M., Jr., Carter, A. P., Morgan-Warren, R. J., Wimberly, B. T., and Ramakrishnan, V. (2000) The structural basis for the action of the antibiotics tetracycline, pactamycin, and hygromycin B on the 30S ribosomal subunit. *Cell 103*, 1143–1154.
12. Pioletti, M., Schlünzen, F., Harms, J., Zarivach, R., Gluhmann, M., Avila, H., Bashan, A., Bartels, H., Auerbach, T., Jacobi, C., Hartsch, T., Yonath, A., and Franceschi, F. (2001) Crystal structures of complexes of the small ribosomal subunit with tetracycline, edeine and IF3. *EMBO J. 20*, 1829–1839.
13. Aleksandrov, A., and Simonson, T. (2008) Molecular dynamics simulations of the 30S ribosomal subunit reveal a preferred tetracycline binding site. *J. Am. Chem. Soc. 130*, 1114–1115.
14. Mui, S., Delaria, K., and Jurnak, F. (1990) Preliminary crystallographic analysis of a complex between tetracycline and the trypsin-modified form of *Escherichia coli* elongation factor Tu. *J. Mol. Biol. 212*, 445–447.
15. Krab, I. M., and Parmeggiani, A. (2002) Mechanisms of EF-Tu, a pioneer GTPase. *Prog. Nucleic Acids Res. Mol. Biol. 71*, 513–551.
16. Parmeggiani, A., Krab, I. M., Okamura, S., Nielsen, R. C., Nyborg, J., and Nissen, P. (2006) Structural basis of the action of pulvomycin and GE2270 A on elongation factor Tu. *Biochemistry 45*, 6846–6857.
17. Zuurmond, A.-M., Olsthoorn-Tieleman, L. N., de Graaf, J. M., Parmeggiani, A., and Kraal, B. (1999) Mutant EF-Tu species reveal novel features of the enacyloxin IIa inhibition mechanism on the ribosome. *J. Mol. Biol. 294*, 627–637.
18. Heffron, S. E., Mui, S., Aorora, A., Abel, K., Bergmann, E., and Jurnak, F. (2006) Molecular complementarity between tetracycline and the GTPase active site of elongation factor Tu. *Acta Crystallogr. D62*, 1392–1400.
19. Kollman, P., Massova, I., Reyes, C., Kuhn, B., Huo, S., Chong, L., Lee, M., Lee, T., Duan, Y., Wang, W., Donini, O., Cieplak, P., Srinivasan, J., Case, D., and Cheatham, T. (2000) Calculating structures and free energies of complex molecules: Combining molecular mechanics and continuum models. *Acc. Chem. Res. 33*, 889–897.
20. Jorgensen, W. (2003) The many roles of computation in drug discovery. *Science 303*, 1813–1818.
21. McCammon, J. (2005) Computation of noncovalent binding affinities. In *Theory and Applications of Computational Chemistry* (Dykstra, C., Frenking, G., Kim, K., and Scuseria, G., Eds.) pp 41−46, Elsevier, Amsterdam.
22. Becker, O. M., MacKerell, A. D., Jr., Roux, B., and Watanabe, M., Eds. (2001) *Computational Biochemistry & Biophysics*, Marcel Dekker, New York.
23. Simonson, T., Archontis, G., and Karplus, M. (2002) Free energy simulations come of age: The protein−ligand recognition problem. *Acc. Chem. Res. 35*, 430–437.
24. Simonson, T. (2006) Free energy calculations: Approximate methods for biological macromolecules. In *Free energy calculations: Theory and applications in chemistry and biology* (Chipot, C., and Pohorille, A., Eds.) Chapter 12, Springer-Verlag, New York.
25. Aleksandrov, A., and Simonson, T. (2006) The tetracycline:Mg^{2+} complex: A molecular mechanics force field. *J. Comput. Chem. 13*, 1517–1533.
26. Aleksandrov, A., Schuldt, L., Hinrichs, W., and Simonson, T. (2008) Tet repressor induction by tetracycline: A molecular dynamics, continuum electrostatics, and crystallographic study. *J. Mol. Biol. 378*, 896–910.
27. Ross, J., Eady, E., Cove, J., and Cunliffe, W. (1998) 16S rRNA mutation associated with tetracycline resistance in a Gram-positive bacterium. *Antimicrob. Agents Chemother. 42*, 1702–1705.
28. Trinh, H., Billington, S., Field, A., Songer, J., and Jost, B. (2002) Susceptibility of *Arcanobacterium pyogenes* from different sources to tetracycline, macrolide and lincosamide antimicrobial agents. *Vet. Microbiol. 85*, 353–359.
29. Bergeron, J., Ammirati, M., Danley, D., James, L., Norcia, M., Retsema, J., Strick, C., Su, W., Sutcliffe, J., and Wondrack, L. (1996) Glycylcyclines bind to the high-affinity tetracycline ribosomal binding site and evade Tet(M)- and Tet(O)-mediated ribosomal protection. *Antimicrob. Agents Chemother. 40*, 2226–2228.
30. Olson, M. W., Ruzin, A., Feyfant, E., Rush, T. S., O'Connell, J., and Bradford, P. A. (2006) Functional, biophysical, and structural bases for antibacterial activity of tigecycline. *Antimicrob. Agents Chemother. 50*, 2156–2166.
31. Failing, K., Theis, P., and Kaleta, E. (2006) Determination of the inhibitory concentration 50% (IC50) of four selected drugs (chlortetracycline, doxycycline, enrofloxacin and difloxacin) that reduce in vitro the multiplication of *Chlamydophila psittaci*. *Dtsch. Tieraerztl. Wochenschr. 113*, 412–417.
32. Aleksandrov, A., Proft, J., Hinrichs, W., and Simonson, T. (2007) Protonation patterns in tetracycline:Tet repressor recognition: Simulations and experiments. *ChemBioChem 8*, 675–685.
33. Abel, K., Yoder, M. D., Hilgenfeld, R., and Jurnak, F. (1996) An α to β conformational switch in EF-Tu. *Structure 4*, 1153–1159.
34. Beglov, D., and Roux, B. (1994) Finite representation of an infinite bulk system: Solvent boundary potential for computer simulations. *J. Chem. Phys. 100*, 9050–9063.
35. Simonson, T. (2000) Electrostatic free energy calculations for macromolecules: A hybrid molecular dynamics/continuum electrostatics approach. *J. Phys. Chem. B 104*, 6509–6513.
36. Nina, M., and Simonson, T. (2002) Molecular dynamics of the $tRNA^{Ala}$ acceptor stem: Comparison between continuum reaction field and particle-mesh Ewald electrostatic treatments. *J. Phys. Chem. B 106*, 3696–3705.
37. Mackerell, A., Bashford, D., Bellott, M., Dunbrack, R., Evanseck, J., Field, M., Fischer, S., Gao, J., Guo, H., Ha, S., Joseph, D., Kuchnir, L., Kuczera, K., Lau, F., Mattos, C., Michnick, S., Ngo, T., Nguyen, D., Prodhom, B., Reiher, W., Roux, B., Smith, J., Stote, R., Straub, J., Watanabe, M., Wiorkiewicz-Kuczera, J., Yin, D., and Karplus, M. (1998) An all-atom empirical potential for molecular modelling and dynamics study of proteins. *J. Phys. Chem. B 102*, 3586–3616.
38. Jorgensen, W., Chandrasekar, J., Madura, J., Impey, R., and Klein, M. (1983) Comparison of simple potential functions for simulating liquid water. *J. Chem. Phys. 79*, 926–935.

39. Stote, R., States, D., and Karplus, M. (1991) On the treatment of electrostatic interactions in biomolecular simulation. *J. Chim. Phys. 88*, 2419–2433.
40. Brooks, B., Bruccoleri, R., Olafson, B., States, D., Swaminathan, S., and Karplus, M. (1983) Charmm: A program for macromolecular energy, minimization, and molecular dynamics calculations. *J. Comput. Chem. 4*, 187–217.
41. Guymon, R., Pomerantz, S. C., Crain, P. F., and McCloskey, J. A. (2006) Influence of phylogeny on posttranscriptional modification of rRNA in thermophilic prokaryotes: The complete modification map of 16S rRNA of *Thermus thermophilus*. *Biochemistry 45*, 4888–4899.
42. Simonson, T. (2001) Free energy calculations. In *Computational Biochemistry & Biophysics* (Becker, O., Mackerell, A., Jr., Roux, B., and Watanabe, M., Eds.) Chapter 9, Marcel Dekker, New York.
43. Thompson, D., Plateau, P., and Simonson, T. (2006) Free energy simulations reveal long-range electrostatic interactions and substrate-assisted specificity in an aminoacyl-tRNA synthetase. *ChemBioChem 7*, 337–344.
44. Thompson, D., and Simonson, T. (2006) Molecular dynamics simulations show that bound Mg^{2+} contributes to amino acid and aminoacyl adenylate binding specificity in aspartyl-tRNA synthetase through long range electrostatic interactions. *J. Biol. Chem. 281*, 23792–23803.
45. Sagui, C., and Darden, T. (1999) Molecular dynamics simulations of biomolecules: Long-range electrostatic effects. *Ann. Rev. Biophys. Biomol. Struct. 28*, 155–179.
46. Hodel, A., Simonson, T., Fox, R. O., and Brünger, A. T. (1993) Conformational substates and uncertainty in macromolecular free energy calculations. *J. Phys. Chem. 97*, 3409–3417.
47. Reinhardt, W., Miller, M., and Amon, L. (2001) Why is it so difficult to simulate entropies, free energies, and their differences? *Acc. Chem. Res. 34*, 607–614.
48. Shirts, M. R., Pitera, J. W., Swope, W. C., and Pande, V. S. (2003) Extremely precise free energy calculations of amino acid side chain analogs: Comparison of common molecular mechanics force fields for proteins. *J. Chem. Phys. 119*, 5740–5761.
49. Hermans, J. (1991) Simple analysis of noise and hysteresis in (slow-growth) free energy simulations. *J. Phys. Chem. 95*, 9029–9032.
50. Wood, R. H. (1991) Estimation of errors in free energy calculations due to the lag between the Hamiltonian and the system configuration. *J. Phys. Chem. 95*, 4838–4842.
51. Hummer, G. (2001) Fast growth thermodynamic integration: Error and efficiency analysis. *J. Chem. Phys. 114*, 7330–7337.
52. Thompson, D., Lazennec, C., Plateau, P., and Simonson, T. (2007) Ammonium scanning in an enzyme active site: The chiral specificity of aspartyl-tRNA synthetase. *J. Biol. Chem. 42*, 30856–30868.
53. Straatsma, T., Berendsen, H., and Stam, A. (1986) Estimation of the statistical error in molecular simulation calculations. *Mol. Phys. 57*, 89–95.
54. Allen, M., and Tildesley, D. (1991) *Computer Simulations of Liquids*, Clarendon Press, Oxford, U.K.
55. Sham, Y., Chu, Z., and Warshel, A. (1997) Consistent calculations of pK_a's of ionizable residues in proteins: Semi-microscopic and microscopic approaches. *J. Phys. Chem. B 101*, 4458–4472.
56. Eberini, I., Baptista, A., Gianazza, E., Fraternali, F., and Beringhelli, T. (2004) Reorganization in apo- and holo-β-lactoglobulin upon protonation of Glu89: Molecular dynamics and pK_a calculations. *Proteins 54*, 744–758.
57. Archontis, G., and Simonson, T. (2005) Proton binding to proteins: A free energy component analysis using a dielectric continuum model. *Biophys. J. 88*, 3888–3904.
58. Tembe, B., and McCammon, J. (1984) Ligand-receptor interactions. *Comput. Chem. 8*, 281–283.
59. Kollman, P. (1993) Free energy calculations: Applications to chemical and biochemical phenomena. *Chem. Rev. 93*, 2395.
60. Greenwald, R. A., Hillen, W., and Nelson, M. L. (2001) *Tetracyclines in Biology, Chemistry and Medicine*, Birkhäuser Verlag, Basel, Switzerland.
61. Foloppe, N., and MacKerell, A. D., Jr. (2000) Parameter optimization based on small molecule and condensed phase macromolecular target data. *J. Comput. Chem. 21*, 86–104.
62. Gromadski, K., Wieden, H.-J., and Rodnina, M. (2002) Kinetic mechanism of Elongation Factor Ts-catalyzed nucleotide exchange in Elongation Factor Tu. *Biochemistry 41*, 162–169.
63. Aleksandrov, A., and Simonson, T. (2008) Molecular mechanics models for tetracycline analogs. *J. Comput. Chem.* (in press).
64. Archontis, G., Simonson, T., and Karplus, M. (2001) Binding free energies and free energy components from molecular dynamics and Poisson-Boltzmann calculations. Application to amino acid recognition by aspartyl-tRNA synthetase. *J. Mol. Biol. 306*, 307–327.
65. Hendsch, Z., and Tidor, B. (1999) Electrostatic interactions in the GCN4 leucine zipper: Substantial contributions arise from intramolecular interactions enhanced on binding. *Protein Sci. 8*, 1381–1392.
66. Scholz, O., Kostner, M., Reich, M., Gastiger, S., and Hillen, W. (2003) Teaching TetR to recognize a new inducer. *J. Mol. Biol. 329*, 217–227.
67. Boucher, H. W., Wennersten, C. B., and Eliopoulos, G. M. (2000) In vitro activities of the glycylcycline GAR-936 against gram-positive bacteria. *Antimicrob. Agents Chemother. 44*, 2225–2229.
68. Chopra, I. (2002) New developments in tetracycline antibiotics: Glycylcyclines and tetracycline efflux pump inhibitors. *Drug Resist. Updates 5*, 119–125.
69. Bauer, G., Berens, C., Projan, S. J., and Hillen, W. (2004) Comparison of tetracycline and tigecycline binding to ribosomes mapped by dimethylsulphate and drug-directed Fe^{2+} cleavage of 16S rRNA. *J. Antimicrob. Chemother. 53*, 592–599.
70. Pringle, M., Fellstrom, C., and Johansson, K. E. (2007) Decreased susceptibility to doxycycline associated with a 16S rRNA gene mutation in *Brachyspira hyodysenteriae*. *Vet. Microbiol. 123*, 245–248.
71. Wong, C., and McCammon, J. (2003) Protein simulation and drug design. *Adv. Protein Chem. 66*, 87–121.
72. Mackerell, A., Wiorkiewicz-Kuczera, J., and Karplus, M. (1995) An all-atom empirical energy force-field for the study of nucleic acids. *J. Am. Chem. Soc. 117*, 11946–11975.
73. Hinrichs, W., Kisker, C., Duvel, M., Muller, A., Tovar, K., Hillen, W., and Saenger, W. (1994) Structure of the Tet repressor-tetracycline complex and regulation of antibiotic resistance. *Science 264*, 418–420.
74. Saenger, W., Orth, P., Kisker, C., Hillen, W., and Hinrichs, W. (2000) The tetracycline repressor: A paradigm for a biological switch. *Angew. Chem., Int. Ed. 39*, 2042–2052.

BI801726Q